

ASSESSING MODEL STRUCTURE UNCERTAINTY THROUGH AN ANALYSIS OF SYSTEM FEEDBACK AND BAYESIAN NETWORKS

GEOFFREY R. HOSACK,^{1,3} KEITH R. HAYES,² AND JEFFREY M. DAMBACHER²

¹*Department of Fisheries and Wildlife, Oregon State University, 104 Nash Hall, Corvallis, Oregon 97331 USA*

²*CSIRO Mathematical and Information Sciences, GPO Box 1538, Hobart, Tasmania 7001, Australia*

Abstract. Ecological predictions and management strategies are sensitive to variability in model parameters as well as uncertainty in model structure. Systematic analysis of the effect of alternative model structures, however, is often beyond the resources typically available to ecologists, ecological risk practitioners, and natural resource managers. Many of these practitioners are also using Bayesian belief networks based on expert opinion to fill gaps in empirical information. The practical application of this approach can be limited by the need to populate large conditional probability tables and the complexity associated with ecological feedback cycles. In this paper, we describe a modeling approach that helps solve these problems by embedding a qualitative analysis of sign directed graphs into the probabilistic framework of a Bayesian belief network. Our approach incorporates the effects of feedback on the model's response to a sustained change in one or more of its parameters, provides an efficient means to explore the effect of alternative model structures, mitigates the cognitive bias in expert opinion, and is amenable to stakeholder input. We demonstrate our approach by examining two published case studies: a host–parasitoid community centered on a nonnative, agricultural pest of citrus cultivars and the response of an experimental lake mesocosm to nutrient input. Observations drawn from these case studies are used to diagnose alternative model structures and to predict the system's response following management intervention.

Key words: *Bayesian belief network; expert opinion; feedback; model uncertainty; risk assessment; signed directed graphs.*

INTRODUCTION

Ecologists, natural resource managers, and practitioners of ecological risk assessment operate in complex and often poorly understood settings. Each is forced to design experiments, make predictions, or assess decisions without completely understanding the underlying processes, structure, and dynamics of complex ecosystems (Francis and Shotton 1997, Ruckelshaus et al. 2002, Fairbrother and Turnley 2005). The predictive, numeric, process-based models that each employs typically address parametric uncertainty using Monte Carlo simulations (Metropolis and Ulam 1949). However, process-based models of ecological systems inevitably have many possible alternative structures. A systematic analysis of the effects of different model structures is often not practicable with the limited resources available for any single study (Hoffman and Hammonds 1994, Reckhow 1994, Ferson 1996), despite the fact that ecological predictions and management strategies may be more sensitive to the structural uncertainty of a model than parametric uncertainty (Punt and Hilborn 1997, Varis and Kuikka 1999, Dambacher et al. 2002).

Besides the problem of choosing an appropriate model structure, practitioners of ecological risk assessment and natural resource managers, when faced with insufficient quantitative knowledge to adequately capture parametric uncertainty, typically eschew quantitative analysis methods in favor of methods based on expert opinion (see Burgman 2005:381; Office of the Gene Technology Regulator 2005:25). A popular way to fill gaps in empirical information is to incorporate expert opinion into a Bayesian belief network, or BBN (Varis and Kuikka 1999, Marcot et al. 2001, Borusk et al. 2004, Pollino et al. 2007). Without empirical data, however, experts must, in what could be a laborious and time-consuming process, specify the relevant conditional probabilities in the BBN (Ticehurst et al. 2007). Furthermore, expert opinion can be subject to cognitive bias unless carefully elicited (Morgan and Henrion 1990, Burgman 2005), and might be further confounded by linguistic uncertainty (Regan et al. 2002). Another difficulty is that including feedbacks via cyclic network structures requires dynamic time-explicit BBNs that depend on extensive parameterization (Burger and Gochfeld 1997, Ong et al. 2002, Borusk et al. 2004, Dojer et al. 2006). Hence, BBNs based on expert opinion do not usually include feedbacks common to ecological systems in their network structure (e.g., Marcot et al. 2001, Stiber et al. 2004).

Manuscript received 21 March 2007; revised 26 October 2007; accepted 4 December 2007. Corresponding Editor: J. A. Powell.

³ E-mail: geoff.hosack@oregonstate.edu

Here we present a method that addresses the problems highlighted above by merging BBNs with another form of graphical model used in ecology: signed directed graphs (Levins 1974, Dambacher et al. 2002, 2003b). This new method incorporates feedback and facilitates comparison of alternative model structures and thereby provides a practical way to explore the effects of model structure uncertainty in complex ecosystems. This method is designed to assist ecologists, risk practitioners, and natural resources managers in predicting how ecosystems might respond to a disturbance, in exploring the dynamics of alternative model structures, in performing model diagnosis, and in optimizing the allocation of resources for monitoring programs. It also reduces the need for experts to estimate complex conditional probabilities, thereby limiting opportunities for the introduction of cognitive bias into the BBN.

MATERIALS AND METHODS

Analyzing the effect of press perturbations

Bayesian belief networks allow the probabilistic representation of a system based on multiple sources of knowledge. The conditional relationships between a system’s variables (nodes) are visually depicted using directed acyclic graphs, DAGs (Pearl 2000). By definition, a directed acyclic graph lacks feedback; that is, a path traced along its links cannot pass through a variable more than once. Signed directed graphs (SDGs), however, can incorporate feedback cycles, provide predictions of increase (+), decrease (−), or no change (0) for specified variables, and can quickly evaluate the consequences of alternative model structures (Levins 1974, Dambacher et al. 2002).

Just as the DAG graphically describes the probabilistic relationships within a Bayes network, the SDG describes an underlying deterministic, mathematical model. The model underlying a SDG describes the dynamics of n number of variables X_i in a system of differential equations:

$$\frac{dX_i}{dt} = f_i(X_1, \dots, X_n; p_1, \dots, p_k) \quad i = 1 \dots n \quad k = 1 \dots m \quad (1)$$

where m number of parameters p_k control the rates of increase or decrease. The Jacobian matrix \mathbf{A} is composed of the first partial derivatives of the growth functions f_i taken with respect to the variables and evaluated at equilibrium, such that

$$a_{ij} = \left. \frac{\partial f_i}{\partial X_j} \right|_* \quad (2)$$

where * denotes evaluation at equilibrium (May 1974).

Both the SDG and the matrix \mathbf{A} represent the qualitative relationship between variables in a model ecosystem (Levins 1974). A three-variable SDG model (Fig. 1) translated into matrix form is as follows:

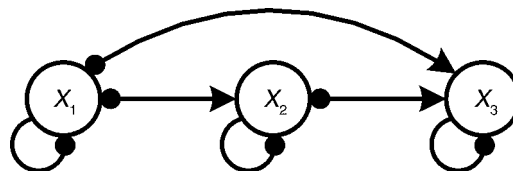


FIG. 1. Signed directed graph (SDG) depicting a top predator X_3 consuming prey X_1 and X_2 from two different trophic levels. Negative direct effects are shown by lines ending in a solid circle, and positive direct effects are depicted with arrows. Intraspecific density-dependent processes are represented by a line returning to the source variable.

$$\mathbf{A} = \begin{bmatrix} -a_{1,1} & -a_{1,2} & -a_{1,3} \\ a_{2,1} & -a_{2,2} & -a_{2,3} \\ a_{3,1} & a_{3,2} & -a_{3,3} \end{bmatrix}$$

where the matrix entry in the i th row and the j th column shows the magnitude (a_{ij}), and the sign (+, −) of the direct effect of variable j on variable i . The rows are the receiving variables and the columns are the source variables of the direct effects shown in Fig. 1. For example, the direct effect of X_3 on X_2 is negative and is represented by $-a_{2,3}$ since the predator imparts mortality to its prey.

A sustained change to a parameter, referred to here as a “press perturbation” (Bender et al. 1984), will shift the system to a new equilibrium. The average values of the system’s variables at this new equilibrium point (which variously may have increased, decreased, or remained unchanged) can be estimated by inverting the negative of the matrix \mathbf{A} in the following equation:

$$\frac{\partial \mathbf{X}^*}{\partial p_k} = -\mathbf{A}^{-1} \frac{\partial \mathbf{f}}{\partial p_k} \quad (3)$$

where ∂p_k is the parameter shift in the press perturbation, and \mathbf{f} is the vector of growth functions for the system of Eq. 1. The inverse matrix $-\mathbf{A}^{-1}$ accounts for both direct and indirect effects resulting from the press perturbation, and is equivalent to the classical adjoint of $-\mathbf{A}$ divided by its determinant:

$$-\mathbf{A}^{-1} = \frac{\text{adj}(-\mathbf{A})}{\det(-\mathbf{A})} \quad (4)$$

Because $\det(-\mathbf{A})$ is a common denominator for all entries within the adjoint matrix, the long-term direction of change in the levels of the variables X_i following a press perturbation on parameter p_k can be determined by examining elements of the adjoint matrix (Dambacher et al. 2002, 2005). The entries of $\text{adj}(-\mathbf{A})$, are feedback cycles (addends) that are the direct and indirect effects that govern the response of each variable to a press perturbation (Dambacher et al. 2002, 2003a).

Analyzing the qualitative effect of feedback

The elements of a quantitatively specified Jacobian matrix (denoted $\# \mathbf{A}$) contain numerical entries, such as

$$\#A = \begin{bmatrix} -0.9 & -0.8 & -0.7 \\ 0.6 & -0.5 & -0.4 \\ 0.3 & 0.2 & -0.1 \end{bmatrix}$$

Note, however, that n^2 experiments are needed to empirically estimate the magnitude of all entries within **A** (Bender et al. 1984), an arduous task for even a moderately complex system. This clearly limits the applicability of quantitative approaches (Levins 1998). Further, the predictions of numeric matrices can be overly sensitive to the exact values of the matrix entries (Yodzis 1988). For instance, if the magnitude of $a_{1,2}$ in the above system was increased by just 10% to -0.88 , then the prediction given by $-\#A_{1,3}^{-1}$ would shift from a negative to a positive value. Here, we instead focus on a qualitative specification of **A**, and define the matrix $^\circ A$ with entries that are either $+1$, -1 , or 0 , depending on whether a variable acts to increase, decrease, or exert no direct influence on the growth rate of another variable (the matrix $^\circ A$ can be formally defined as a transposed signed adjacency matrix).

The sign of an entry within $\text{adj}(-^\circ A)$ gives the net number of feedback cycles that contribute to a variable's response. It provides a prediction of whether the equilibrium values of a variable will increase, decrease, or remain unchanged following a press perturbation (Dambacher et al. 2002). If the feedback cycles in an adjoint matrix entry are all of the same sign, then the prediction is completely determined. But the prediction sign will be ambiguous if both positive and negative feedback cycles are present. To measure the degree to which there are feedback cycles with countervailing sign, we consider the ratio of the net to the total number of feedback cycles in an adjoint matrix entry. The total number of cycles is calculated by use of an adjacency matrix $^\bullet A$, with entries of $+1$ corresponding to each nonzero entry in the matrix $^\circ A$. A matrix of absolute feedback **T** is calculated by use of the matrix permanent (Minc 1978) in each matrix minor of $^\bullet A$, where $T_{ij} = \text{permanent}(\text{minor}(^\bullet A)_{ij})^T$. The prediction weights associated with elements of the adjoint matrix are given by

$$W = \frac{|\text{adj}(-^\circ A)|}{T}$$

where the arrow superscript is a vectorized matrix operator denoting element-by-element division and “|” denotes absolute value; see Dambacher et al. (2002) for a detailed discussion of these matrix operations.

Elements of **W** range from 0 to 1. A value of zero indicates an equal number of both positive and negative cycles. As prediction weights approach 1 then relatively more cycles are of the same sign, and elements with a weight of exactly 1 have cycles that are all of the same sign. When there are no feedback cycles in a response, such that T_{ij} equals zero, then the variable is predicted to remain unchanged following a press perturbation. In this circumstance the sign of $\text{adj}(-^\circ A)_{ij}$ will be zero and the associated prediction weight is set equal to 1.

Verifying sign determinacy

Dambacher et al. (2003a) tested the sign determinacy of elements within $\text{adj}(-^\circ A)$ by randomly allocating values to a_{ij} from a uniform distribution, and comparing the qualitative predictions from the adjoint matrix with responses calculated from the inverse of quantitatively specified matrices. The sign determinacy of responses (i.e., the proportion of quantitative response signs that have the same sign as the qualitative prediction) with prediction weights ≥ 0.5 was shown to generally exceed 90%; below this threshold the sign determinacy of responses declined to 50% for weighted predictions that approached zero. While these tests of sign determinacy were based on a uniform distribution of random interaction strengths, recent studies emphasize the importance of considering skewed distributions in simulations applied to model ecosystems (Berlow et al. 2004, Emmerson and Yearsley 2004, Wootton and Emmerson 2005).

We evaluated the effect of strong and weak interactions on the sign determinacy of $\text{adj}(-^\circ A)_{ij}$, for the models tested by Dambacher et al. (2003a) (Fig. A1), by randomly allocating values to a_{ij} from four different distributions with markedly different types of skew. We also introduced “trophic dependence” by forcing ecologically realistic trophic transfer efficiencies into each simulation. Trophic relationships occur when a variable X_2 consumes another and thus has a negative direct effect, $-a_{1,2}$, on the prey X_1 . The prey X_1 provides a positive direct effect $a_{2,1}$ on the predator. However, $|a_{2,1}| < |-a_{1,2}|$ because of energetic costs resulting from the metabolization of ingested matter and the typically pyramidal distribution of predator and prey population abundances. We use the notation $\#A$ to denote a simulated matrix with numeric entries. Dependence between $\#a_{1,2}$ and $\#a_{2,1}$ is invoked by first drawing the magnitude of the direct effect of predator on prey, $|\#a_{1,2}|$, from its respective distribution (Fig. 3a). This value of $|\#a_{1,2}|$ is then multiplied by a random variable with a uniform (0, 0.01) distribution that reflects the constraints on density and energy transfer to produce the magnitude of $\#a_{2,1}$. The 0.01 upper limit reflects the assumption that the equilibrium biomass between the prey and its consumer differ 10-fold, and the assumption that maximum ecological efficiency is 10%. Other forms of trophic dependence with different upper limits gave qualitatively similar results (see Appendix for details).

We used Monte Carlo simulations to create 500 stable numeric matrices (May 1974, Dambacher et al. 2003a), where stability was determined by the real parts of all eigenvalues of $\#A$ being negative. We assume that the simulated matrices represent generalized Lotka-Volterra systems with nonzero equilibriums for all species. Separate simulations were done for each model structure under each combination of parameter shape and dependence assumptions.

We examined the proportion of simulations with the “correct” sign, i.e., $\text{sign}(\text{adj}(-^\circ A)_{ij}) = \text{sign}(\text{adj}(-\#A)_{ij})$,

for all elements of adjoint matrices combined across all 18 model systems. We used a least squares fit to the following nonlinear function:

$$\Pr\left\{\text{sign}[\text{adj}(-\circ\mathbf{A})_{ij}] = \text{sign}[\text{adj}(-\#\mathbf{A})_{ij}]\right\} = \frac{\exp(\beta_W \mathbf{W}_{ij} + \beta_{WT} \mathbf{W}_{ij} \mathbf{T}_{ij})}{1 + \exp(\beta_W \mathbf{W}_{ij} + \beta_{WT} \mathbf{W}_{ij} \mathbf{T}_{ij})} \quad (5)$$

Eq. 5 is a logistic-type function that incorporates the influence of prediction weights and absolute feedback on the expected proportion of correct sign. The logistic form allows a flexible curve to be fit to the simulation results with a priori bounds between 0.5 and an upper asymptote of 1.0. The parameter β_W incorporates the direct effect of the prediction weights, and β_{WT} the interaction between prediction weights and total feedback. The intercept at $\mathbf{W}_{ij}=0$ is fixed at a value of 0.5 to impose an equal chance of the response being either positive or negative when it is composed of an equal number of positive and negative feedback cycles contributing to a response. Note that a variety of different functions could be used to translate the simulation results into the probabilities of having the correct sign (e.g., see Appendix for a 95% lower bound on the proportions of correct sign).

Translating model predictions into conditional probabilities

The transition from SDGs to BBNs is completed by translating the prediction weights associated with each element of $\text{adj}(-\circ\mathbf{A})$ into a probability that is then incorporated into the conditional probability tables of a BBN. A choice needs to be made about how the BBN will be implemented and we suggest two possible conventions. The first preserves the three categories of response predicted by the SDG. That is, in addition to the binary response fit by Eq. 5 for predictions with feedback, there may also be predictions of no change due to a lack of feedback (see *Materials and methods: Analyzing the qualitative effect of feedback*). In this approach, the binary response of Eq. 5 is translated to the three-category conditional probability via the following linear relationship:

$$\Pr\left\{\text{sign}[\text{adj}(-\circ\mathbf{A})_{ij}]\right\} = \frac{4g(\mathbf{W}_{ij}, \mathbf{T}_{ij}) - 1}{3} \quad (6)$$

where $g(\mathbf{W}_{ij}, \mathbf{T}_{ij})$ is the function given by Eq. 5. The remaining probability $1 - \Pr(\text{sign}[\text{adj}(-\circ\mathbf{A})_{ij}])$ must then be divided in some proportion between the two other categories at the analyst’s discretion. In the examples presented here, the remaining probability is simply apportioned equally. For instance, if $\text{adj}(-\circ\mathbf{A})_{ij}$ is negative, then $\Pr(\text{decrease})$ is substituted into the left-hand side of Eq. 6, and the remaining probability $1 - \Pr(\text{decrease})$ is equally apportioned to the categories of increase and no observable (obs.) change. If, however,

$\mathbf{W}_{ij}=0$ and $\mathbf{T}_{ij} > 0$, the SDG is uninformative and Eq. 6 assigns probability equally among the three categories.

The second convention allows the assignment of nonzero observation likelihoods only to the categories of increase or decrease, and Eq. 5 is applied without the linear transformation in Eq. 6 to give probabilities of increase and decrease. If $\mathbf{W}_{ij} = 0$ and $\mathbf{T}_{ij} > 0$, Eq. 5 automatically allocates equal probability to increase and decrease. The implications of these two conventions are discussed further in *Discussion*.

From signed directed graphs to Bayesian belief networks

Here we embed the consequences of cyclical SDGs into the conditional probabilities of an acyclic BBN (Fig. 2). Each variable in the SDG has a corresponding observation–prediction node that denotes a set of conditional probabilities (a conditional probability table; CPT) in the BBN. For a given SDG, Eqs. 5 and 6 are used to estimate the probability of predicted response for all possible inputs (press perturbations) to the SDG. The CPTs within the observation–prediction nodes record the probability of observing an increase, decrease, or no apparent response conditional on (1) l input nodes that have probabilities of positive input, negative input, or no input where l is the number of variables in the SDG that are subject to a press perturbation; and, (2) a structure node that represents all alternative model structures (SDGs) that describe the system. We define the probability of a model being “true” as the degree to which it is consistent with observations relative to the other alternative models. It is always possible, however, that none of the SDGs accurately depict the sign response of the system in question. A “null model” is therefore introduced as a benchmark to judge the performance of the SDGs. The null model allocates equal probabilities of observing an increase, decrease, or no response across every possible prediction given a press perturbation, and is structurally equivalent to a fully connected matrix (i.e., an $n \times n$ matrix \mathbf{A} filled with +1’s). For details on the process of constructing BBNs from conditional probabilities see, for example, Cain (2001).

RESULTS

Verifying sign determinacy

Our results showed that prediction weights are informative when strong and weak interactions, and ecologically realistic trophic transfer efficiencies (i.e., trophic dependence) are introduced into the simulations. Sign determinacy was strongly related to prediction weights (\mathbf{W}_{ij}) for all parameter distribution shapes and forms of dependence tested (Fig. 3). Moreover, sign determinacy of $\text{adj}(-\circ\mathbf{A})_{ij}$ for a given prediction weight was found to increase as a function of the absolute number of feedback cycles (\mathbf{T}_{ij}). The parameters β_W and β_{WT} were highly significant for all fits (Appendix: Table A1).

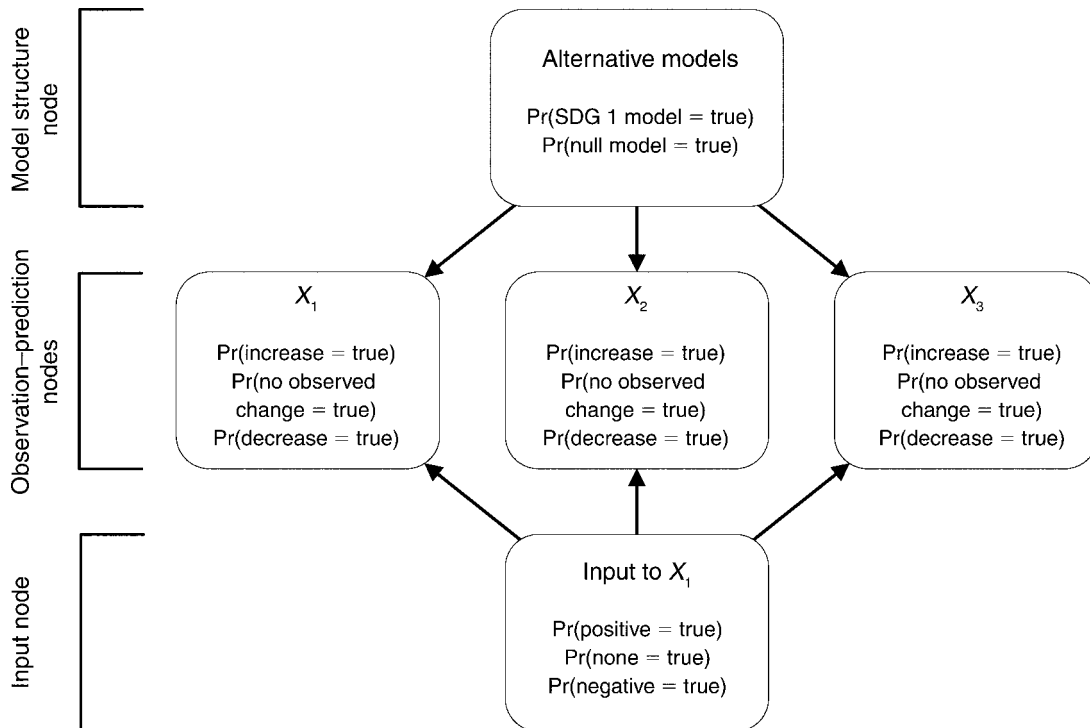


FIG. 2. Bayesian belief network of the signed directed graph model from Fig. 1 (SDG 1) and competing null model. A press perturbation is made only on variable X_1 .

Introducing trophic dependence among the elements of **A** had a much greater effect on sign determinacy than did the skewness of the distribution of interaction strengths. The relative frequency of strong and weak links, described by the different distribution types, was relatively unimportant and had only a minor effect on the fitted values of β_W and β_{WT} . Conversely, trophic dependence between the elements of matrix **A** introduced a nonrandom pattern of weak interaction strengths that diminished the proportion of correct qualitative predictions (Fig. 3c), and increased the standard error of β_W and β_{WT} (Appendix: Table A1). Even with this increased scatter, however, the parameters of Eq. 5 remained significant, and therefore informative, under all the scenarios examined in our simulations. In the succeeding examples, we employ the fit of Eq. 5 with trophic dependency and uniformly distributed magnitudes of interactions (Fig. 3c, top) to generate the conditional probability tables for the example BBNs. In the Appendix, we provide a more conservative alternative to Eq. 5 for calculating proportion of correct sign, and apply a 95% lower bound to the points in Fig. 3c.

Example applications

The red scale *Aonidiella aurantii* is a common nonnative insect pest of orange, grapefruit, and lemon crops in California. The red scale is parasitized by two nonnative wasps *Encarsia perniciosi* and *Aphytis meli-*

nus. A SDG of this host-parasitoid community is identical to the model introduced in Fig. 1. Rather than explicitly including the three species of scale insect and wasps, we identify three variables describing different states of parasitization among the red scale host: unparasitized hosts (X_1), hosts parasitized by *E. perniciosi* (X_2), and hosts parasitized by *A. melinus* (X_3). Unparasitized hosts are transferred into a parasitized state following an attack by either *E. perniciosi* or *A. melinus*. These parasitoids are assumed to attack scale hosts at a rate proportional to the number of scale hosts already parasitized; this produces a predator-prey type relationship of parasitized hosts on their "prey," the unparasitized hosts. In another predator-prey type relationship, attacks by *A. melinus* on scale hosts already parasitized by *E. perniciosi* are assumed to transfer these hosts into a state of parasitization by *A. melinus* (Borer et al. 2003, 2004). All three variables exhibit intraspecific density-dependent growth; for unparasitized hosts it is via intraspecific competition for the basal citrus resource (Borer et al. 2003); for hosts parasitized by *A. melinus* and *E. perniciosi*, it is via intraspecific reattack on previously parasitized hosts (Murdoch et al. 2005). The underlying system of equations for this host-parasitoid community model and instructions for constructing the associated BBN are given in the Supplement. We use a BBN to test whether the host-parasitoid community (H-PC) model is consistent with the observational results of Borer et al. (2003). The corresponding BBN

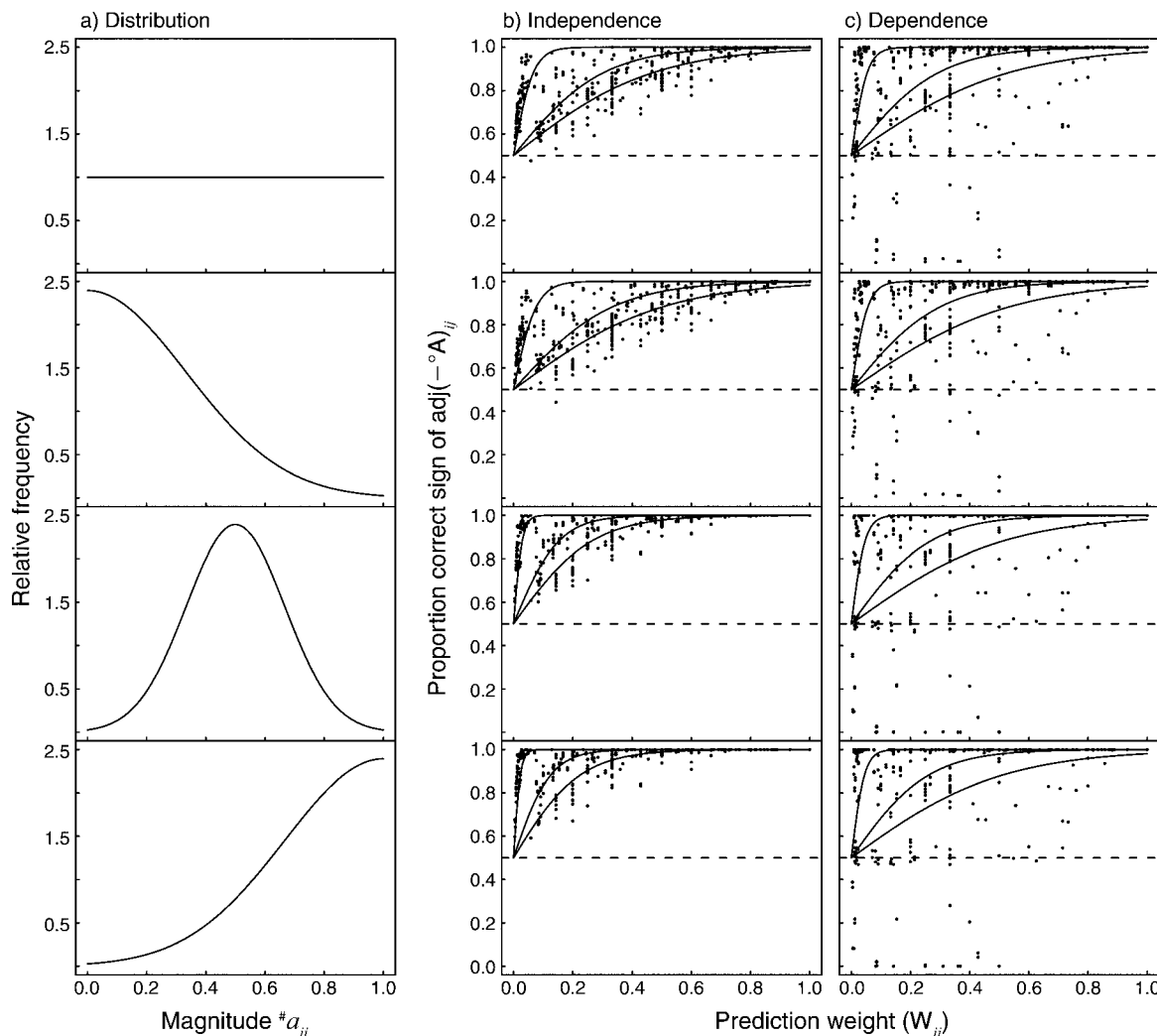


FIG. 3. (a) The four different distributions used to simulate the relative frequency of strong and weak interactions, denoted $^{\#}a_{ij}$, given by the magnitudes of the entries within the numeric Jacobian matrix $^{\#}\mathbf{A}$. Five hundred stable $^{\#}\mathbf{A}$ matrices were simulated for each of 18 different community models (Appendix: Fig. A1). (b) The proportion of qualitative response predictions with the same sign as the quantitative response predictions are plotted against the prediction weight of the qualitative model. The sign of predicted responses are given by entries within the classical adjoint, denoted adj , of the qualitative matrix reversed in sign, $-^{\circ}\mathbf{A}$. The simulated quantitative response predictions are similarly given by $\text{adj}(-^{\#}\mathbf{A})_{ij}$. The magnitudes of the interactions, $^{\#}a_{ij}$, were drawn independently from each of the distributions in panel (a). Each point represents the proportion of simulations with signs correctly predicted by the qualitative model for a particular interaction. The fitted curves are the expected correct proportion given prediction weight and total feedback (Eq. 5; Appendix: Table A1), for three values of total feedback, \mathbf{T} (from bottom to top): $\mathbf{T}_{ij} = 10$, $\mathbf{T}_{ij} = 100$, $\mathbf{T}_{ij} = 1000$. (c) As in (b), but with the $^{\#}a_{ij}$ of predator–prey relationships conditionally dependent such that if the prey is species i and the predator species j , then $0 < ^{\#}a_{ji} < 0.01 \times ^{\#}a_{ij}$, where the $^{\#}a_{ij}$ are drawn independently from the distribution in the corresponding row of panel (a) (see Appendix). Non-trophic $^{\#}a_{ij}$ are drawn independently from the distribution in the corresponding row of panel (a). Note that points are overlapping.

has three observation–prediction nodes, an input node, and a model structure model node (Fig. 4). The performance of the H–PC model is judged against the null model.

We begin by allocating equal prior probabilities to the H–PC model and the null model within the model structure node. Setting the probability of a positive press perturbation, or input, to the scale pest X_1 equal to 1.0 represents an unequivocal increase in the reproductive

rate of unparasitized scale pests (Fig. 4a). In practice this could correspond to regional increase in red scale reproduction across grapefruit, orange, and lemon crops (Borer et al. 2003). If the number of red scale hosts that are parasitized by *A. melinus* (X_3) was observed to increase, then the H–PC model becomes more likely than the null model, i.e., $\text{Pr}(\text{H–PC model is true}) = 0.74$. Given this updated information, the BBN now predicts that unparasitized hosts have an 80% chance of increase

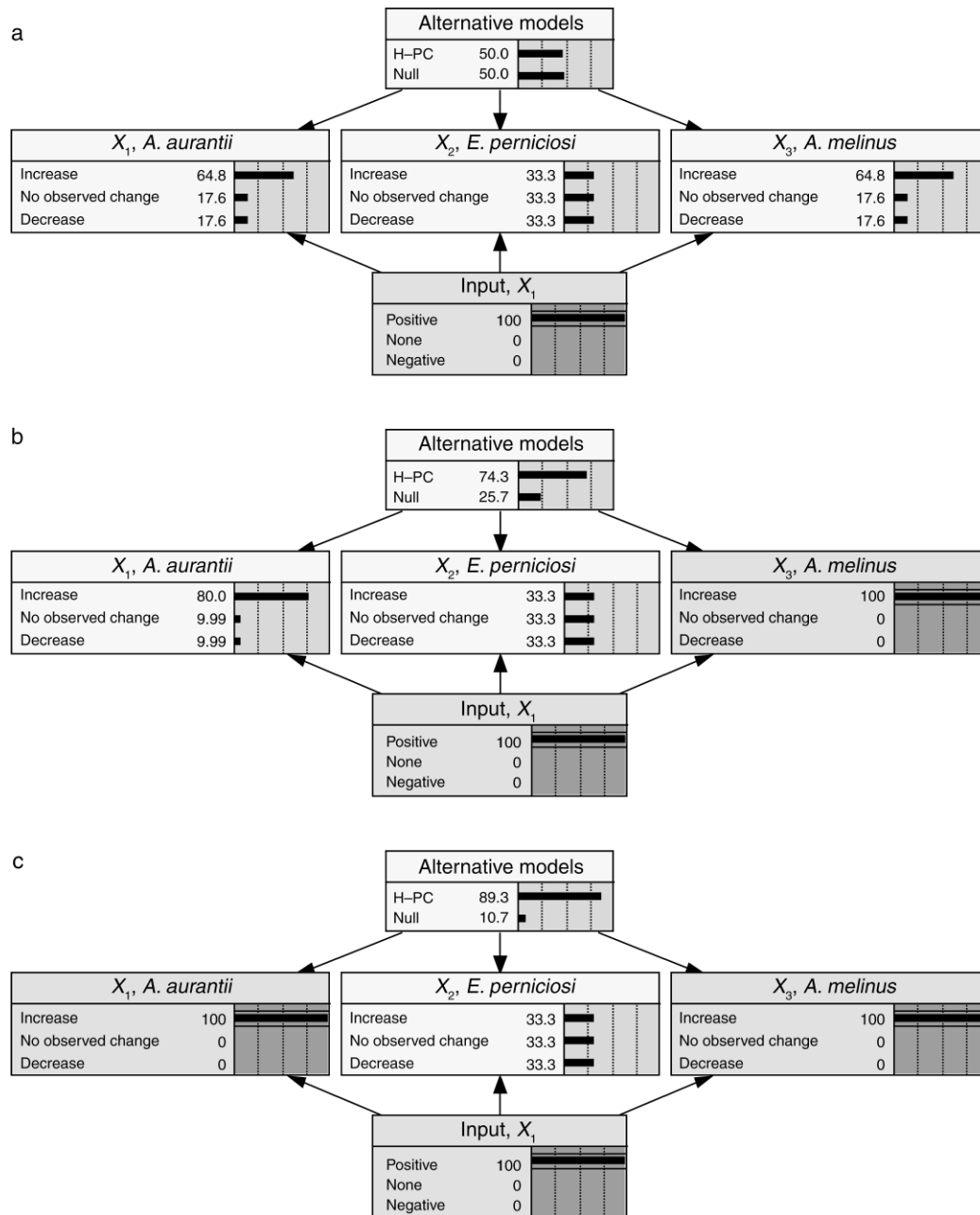


FIG. 4. Bayesian belief network of the Californian red scale pest community (Borer et al. 2003), where X_1 is unparasitized red scale (*Aonidiella aurantii*), X_2 is red scale parasitized by the wasp *Encarsia perniciosi*, and X_3 is red scale parasitized by the wasp *Aphytis melinus*. In this example, there has been a positive input (e.g., increased rate of birth) to unparasitized red scale as shown by 100% chance of a positive input to X_1 . Nodes that have specified observation likelihoods are darker than those that do not. In (a), equal prior probabilities are allocated to the competing models in the structure node. In (b), an observed increase in X_3 supports the H-PC model, thereby increasing the probability of observing an increase in X_1 . In (c), observing an increase in X_1 further supports the H-PC model. BBNs were created using Netica 3.14 (see footnote 4).

whereas before it was 65% (Fig. 4b). Since the H-PC model has been supported, it has contributed more to this subsequent prediction than the null model, and the probability of increase for the density of unparasitized hosts has also risen. If, as in the field observations of Borer et al. (2003), the density of unparasitized hosts

was also observed to increase, then the estimated probability that the H-PC model is true increases to 0.89 (Fig. 4c). Note how the density of red scale parasitized by *E. perniciosi* remains ambiguous (equal probability of observing increase, decrease, or no change) and is therefore uninformative.

TABLE 1. Sensitivity analysis of the agricultural pest Bayesian belief network (BBN) given a positive input to X_1 .

Finding node	Mutual information
Alternative models	1.00
X_1	0.36
X_3	0.36
X_2	0.00

Notes: High values indicate shared information between the structure node and a finding at a node; the structure node in such a case is sensitive to findings at that node (see footnote 4). Sensitivity analysis uses the change in mutual information between two nodes due to the reduction of entropy in node X because of a finding at node Y . The expected reduction in entropy of X due to a finding at Y is zero if X is independent of Y . The mutual information for a finding at the query node Q is the maximum possible for a finding at any node and is included here for scale (boldface).

A researcher, with limited resources, who wishes to test the H-PC model by experimentally increasing red scale reproduction, might ask “What variable should be measured to falsify the H-PC model?” For instance, it may be least costly to measure the density of red scale hosts parasitized by *A. melinus* wasps that develop outside the host (Luck and Podoler 1985), rather than *E. perniciosi* wasps that develop inside the host (Yu et al. 1990). A sensitivity analysis shows how the probabilities of one node are affected by changes made to other nodes; that is, the analysis shows whether or not one node is sensitive to another. A sensitivity analysis on the top node “alternative models” within the BBN (Table 1) suggests that the researcher should measure the density of scale hosts parasitized by *A. melinus* and the density of unparasitized scale hosts. These nodes best discriminate between the hypothesized H-PC model and the null model because they are the most informative: the probabilities of the alternative models are most sensitive to observations made on these variables. Within the context of our qualitative analysis, the researcher would be ill-advised to measure the density of hosts parasitized by *E. perniciosi*, because this variable is uninformative, as both the H-PC and the null model provide equal probabilities of observing an increase, decrease, or no response.

Analyzing the effect of alternative model structures

The previous example compared a single model structure with a null model. Where there are alternative models to be considered with the same number of variables, then it is a straightforward matter to incorporate multiple alternative models in the structure node of the BBN. Here we explore a slightly more complicated BBN structure that allows comparison of SDG models having a different number of variables, and thus a different number of observation-prediction nodes in the BBN. Hulot et al. (2000) explored the ability of alternative SDGs to explain the response of experimental lake mesocosms to nutrient input. Their experimental mesocosms consisted of nutrients (phosphorus) and

three trophic levels: autotrophs, herbivores, and carnivores. They used SDGs to analyze two alternative four-variable food chain models (with assumptions of either prey or ratio dependence) and an eight-variable model based on functional groups (Fig. 5).

We recast the mesocosm lake experiment into an example BBN, and show how it can synthesize empirical data into a common framework facilitating model diagnosis and prediction, as well as suggest management options. We consider a nutrient input into the experimental mesocosm BBN (Fig. 6). First, we use the BBN to predict how variables might respond to the experimental nutrient input if the prey-dependent model or the functional group model is true (Fig. 6a). Second, we use the BBN to determine which model structure may be best supported by the observations (Fig. 6b). As a starting point, the alternative model structures and the null models are assigned equal prior probability within their respective model structure nodes, and an experimental input to phosphorus is assumed.

To incorporate empirical observations, we use the statistical results of Hulot et al. (2000) to assign the likelihood of having observed an increase, decrease, and no response in the levels of the variables. These observation likelihoods may reflect our belief of the applicability of the statistical tests, the power of the tests, interpretation of classical hypothesis testing, and so forth. For purposes of this example, we allocate 100% likelihood that there was an observed increase (decrease) in a variable if the statistical result was classified by Hulot et al. (2000) as significant, and the variable was observed to increase (decrease) in the nutrient-enriched treatment versus the control. If the statistical test was categorized as nonsignificant, then the variable is assumed to have a 100% likelihood of remaining

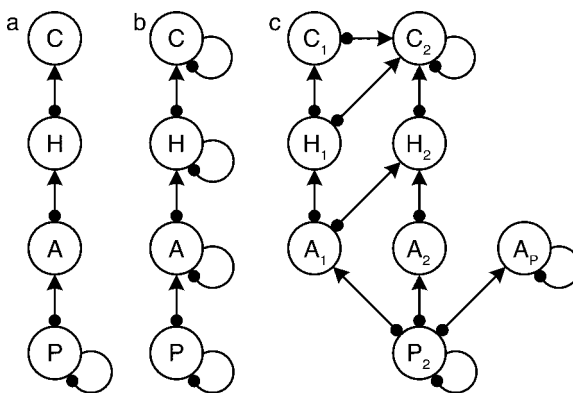


FIG. 5. Alternative model structures of experimental lake mesocosms tested by Hulot et al. (2000). SDG representation of linear trophic food chains with (a) prey dependence, (b) ratio dependence, and (c) a model separating trophic levels into functional groups. Symbols are A, algae; A_1 , edible algae; A_2 , protected algae; A_p , periphyton; C, carnivores; C_1 , invertebrate carnivores; C_2 , fish; H, herbivores; H_1 , small herbivores; H_2 , large herbivores; P, phosphorus. The figure is adapted from Hulot et al. (2000) with permission from Macmillan Publishers, Ltd.

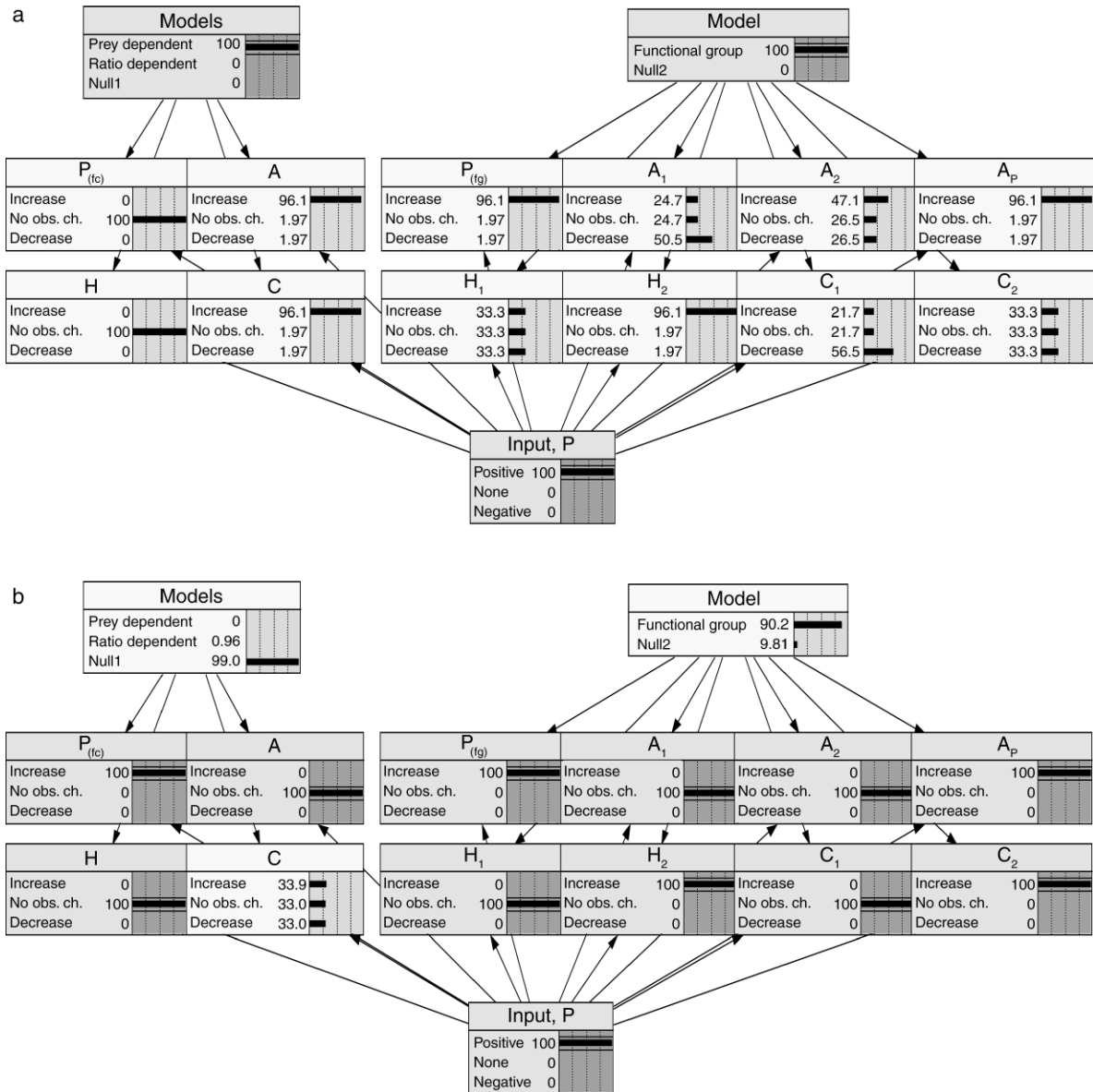


FIG. 6. General structure of Bayesian belief network incorporating both four- and eight-variable SDG models corresponding to Hulot et al.'s (2000) lake mesocosm experiments. Separate structure nodes correspond to the comparison of four variable models and to the comparison of eight variable models. The two structure nodes each have a set of corresponding observation nodes. Since all of the models describe the system's response to the same experimental manipulation, the probability of input to phosphorus is a node common to all observation nodes. Abbreviations are: A, algae; A₁, edible algae; A₂, protected algae; A_P, periphyton; C, carnivores; C₁, invertebrate carnivores; C₂, fish; H, herbivores; H₁, small herbivores; H₂, large herbivores; P_(fc), phosphorus in food chain model; P_(fg), phosphorus in functional group model. In this example, there is a positive input of phosphorus. In (a), prior probabilities are allocated to the competing models in each structure node such that the prey dependence and functional group models have 100% chance of being correct. The predictions of these models are given in the observation-prediction nodes. In (b), the prior probabilities of competing models within each model structure node are given equal probabilities and observation likelihoods are entered as described in *Results: Analyzing the effect of alternative model structures*. Nodes that have specified observation likelihoods are darker than those that do not.

unchanged. While there are a number of ways to assign these likelihoods, our purpose here is simply to demonstrate how observational data can be incorporated into a BBN to yield information on hypothesized model structures.

Sensitivity analysis (Table 2) of the food chain models reveals that, given an unequivocal increase in phosphorus due to an experimental manipulation, monitoring the levels of phosphorus and herbivores would best discriminate between the prey-dependence model, ratio-

dependence model, and null model. Entering into the BBN the observed significant increase in phosphorus and the nonsignificant effect of nutrient enrichment on herbivores updates the probability of the null model being true to about 85%; the alternative models of prey and ratio dependence have a 0% and 15% chance of being true. Including the additional observation of no significant change in algae elevates the estimated probability of the null model being true to 99% (Fig. 6b). Clearly, neither linear food chain model finds much support within the experimental lake mesocosm data observed by Hulot et al. (2000).

Conducting a sensitivity analysis on the functional group model node (Fig. 6), again with an unequivocal increase in phosphorus, suggests that observations on phosphorus (P), large herbivores (H_2), and periphyton (A_P) would best discriminate between the null model and the functional group model (Table 2). Hulot et al. (2000) observed a significant increase in these three variables. Entering these findings into the respective nodes of the BBN gives an estimated probability of about 0.96 that the functional group model is true. The sensitivity analysis also suggests that fish (C_2) and small herbivores (H_1) would not distinguish between alternative model structures. In fact, the response of fish and small herbivores is invariant to the alternative model structures, and observations of these nodes would not improve model diagnosis.

Given these observations the BBN now predicts a 50% chance for a decrease in edible algae (A_1), a 56% chance for a decrease in invertebrate carnivores (C_1), and a 47% chance for an increase in protected algae (A_2). In the lake mesocosms, the observed effect of nutrient enrichment on these three variables was nonsignificant (Hulot et al. 2000). Entering these remaining observations drops the probability that the functional group model is true to 0.90 (Fig. 6b). Although this functional group model is not perfect and, as Hulot et al. (2000) state, there are other conceivable alternative model structures possible, nevertheless, the functional group model appears more consistent with the data compared to either of the food chain models or the null model.

DISCUSSION

Ecologists and natural resource managers often represent impacts to ecological systems as a linear sequence of cause and effect relationships using methods such as fault and event trees (Hayes 2002), path analysis (Shiple 2000), and non-dynamic belief networks (Marcot et al. 2001, Borusk et al. 2004, Pollino et al. 2007). These approaches, however, cannot explicitly account for complex dynamics driven by feedbacks in ecological systems. Feedback cycles can create counterintuitive results that confound predictions and effective management interventions. The modeling framework presented here addresses this problem by embedding the feedback properties of signed directed graphs into the

TABLE 2. Sensitivity analysis of the structure nodes for the BBN in Fig. 6.

Node	Mutual information
Food chain node	
Food chain models	1.585
Phosphorus (food chain), P_{fc}	0.787
Herbivores, H	0.783
Autotrophs, A	0.345
Carnivores, C	0.343
Functional group node	
Functional group models	1.000
Large herbivores, H_2	0.358
Phosphorus (functional groups), P_{fg}	0.358
Periphyton, A_P	0.358
Invertebrate carnivores, C_1	0.039
Edible algae, A_1	0.022
Protected algae, A_2	0.014
Small herbivores, H_1	0.000
Fish, C_2	0.000

Notes: High values indicate increasing shared information between the observation nodes and their respective structure node. The values of the structure nodes serve as a reference (boldface).

conditional probability tables of a Bayesian belief network.

The basic structure of the BBNs used here is relatively simple, yet reflects the essential features of the qualitative dynamics of complex systems in a probabilistic framework. The SDG has a probabilistic interpretation within a BBN that addresses three basic questions.

1) Prediction. What are the probabilities that equilibrium levels will change given a sustained change to a parameter that affects the dynamics of the system? These probabilities are conditional upon (a) the likelihoods of observing an increase, decrease, or no change in the levels of the system's variables, (b) the likelihood of an input to one or more of the system's variables; and, (c) prior belief in model structure.

2) Diagnosis. Which alternative model structure provides predictions that best match the field observations? A model will increase in probability of being true when its predictions are consistent with observations, whereas inconsistent models will decrease in probability. Alternative models are diagnosed based on their probabilities relative to each other and to the null model.

3) Sensitivity. Which nodes are most sensitive to press perturbations on other nodes? Sensitivity analyses deduce the influence of one node on another (e.g., Marcot et al. 2001). This technique is especially useful in deciding which variables to measure or observe in order to distinguish between competing alternative models, and is readily available for use in BBN software packages (e.g., Netica, *available online*).⁴

Incorporating the cyclic behavior of feedback systems within the acyclic framework of a BBN provides a novel

⁴ (www.norsys.com)

way to address uncertainty in the structure of ecological models, and to validate qualitative model predictions with field observations. More importantly, this approach provides an explicit means to record and compare the assumptions that underpin the model and uncertainty in its structure. One of the advantages of this framework is that it eliminates many of the problems associated with traditional BBNs. The conditional probability tables that underlie a BBN must usually be pre-specified by experts, who are set the task of allocating probabilities to an event occurring over an array of varying conditions (Borusk et al. 2004, Ticehurst et al. 2007). For complex BBNs, these tables can be difficult and time consuming to complete. Our approach constructs the conditional probability tables at a key stroke and thereby encourages ecologists and managers to explore a fuller range of alternative model structures and impact scenarios.

The use of the SDG allows continuous time models to inform BBN parameterization. We have used simulations to test the robustness of SDG predictions for an array of network structures to establish a general rule, and provide an alternative to direct parameterization of conditional probabilities by expert opinion (Marcot et al. 2001) or empirical data (Pollino et al. 2007). However, if a particular community structure is of concern, then simulations generated from that model could be used to inform conditional probabilities directly. Implicit is the assumption that dynamics return to approximately steady state between observations. Otherwise, a time-explicit dynamic Bayes network would be required to estimate transient behavior between successive observations. Once the conditional probability tables and the BBN are created, the modularity of BBNs (Mortera et al. 2003, Borusk et al. 2004) allows interconnection with other models developed outside the system described by the SDG. For instance, the lake mesocosm BBN described in the results may be combined into a larger BBN that addresses management options, water quality monitoring programs, and risk pathway analyses.

Our simulation studies allowed us to translate the prediction weights of the SDG into conditional probabilities, and they are based upon the distributions of the interaction strengths and also the structure of the 18 models used in our simulations. Application of these probabilities within the BBN contains an important challenge and a choice among alternative conventions. The challenge is associated with the dependency both in ecological interactions and in feedback cycles. The convention is associated with the two-sign state vs. three-sign state versions of a BBN, with the latter requiring one to choose how to allocate prior probability in the conditional probability tables.

We recognize two forms of dependence that will affect the conditional probabilities derived from the qualitative predictions of the SDG: dependence between pairwise interaction terms (i.e., including but not limited to

trophic dependence) and the dependence created between different elements of the adjoint matrix that have feedback cycles with common combinations of terms (feedback dependence). We discovered that trophic dependence had a greater effect on sign determinacy than the distribution of interaction strengths, but did not seriously undermine the significance and utility of the prediction weights. Feedback dependence is important because it affects the likelihood of multiple observations following an input to the system. In our approach these are treated as independent entities in our BBN structure, but the effect of feedback dependence on the qualitative predictions and diagnosis of alternative model structures, given multiple observations, is in theory available in the SDG and is an avenue for future research.

The practical implications of the convention regarding a two- or three-sign state BBN depends on (1) how observation likelihoods are subsequently entered into the BBN; and (2) how the prior probabilities are allocated in the three state cases. In both conventions, the focus during model diagnosis is on the relative probabilities of alternative models. We have not fully explored the implications of different prior probability assignments and different observational likelihoods for the two conventions. We note that the two conventions produce identical ranks in model diagnosis if prior probability is allocated equally between the two cases not predicted by the SDG (for the three-sign case), and 100% observational likelihood is apportioned to any prediction of increase or decrease. The two conventions may differ, however, if one of the models being compared produces an unambiguous prediction of a zero response. This is because the three-state case can discriminate between uninformative prediction weights (i.e., $\mathbf{W}_{ij} = 0$ and $\mathbf{T}_{ij} > 0$) and unambiguous predictions of no response (i.e., $\mathbf{W}_{ij} = 1$ and $\mathbf{T}_{ij} = 0$), whereas the two-state convention disallows both ambiguous and unambiguous predictions of no response. It is therefore misleading to compare the rank order diagnosis between the two conventions in this situation.

The decision to use the two- or three-state convention depends on the particular application. Under certain circumstances it may be desirable to disallow predictions of zero response, for example, when there is a zero probability of precisely measuring two identical sample means from a continuous probability distribution. It is also easier in the two-state case to assign nonzero observation likelihood across the two categories of increase and decrease. In the three-sign state examples provided here, we have avoided assigning nonzero observation likelihood to more than one category because the effects of such an approach on the rank ordering of alternative models are confounded with the potentially arbitrary prior probability allocations that are necessitated by the three-state case. Thus, in applying the three-state case as developed in this work,

we recommend that the observation likelihood entered for a particular category should be either 0 or 1.0.

Incorporating the graphical BBN and SDG allows the analyst to quickly compare the effects of different model structures. Traditional simulation studies typically emphasize parameter uncertainty rather than model uncertainty (Reckhow 1994, Ferson 1996, Punt and Hilborn 1997, Levins 1998). We do not present this approach as an alternative to traditional simulation studies, but rather as a complement, or precursor, to such studies. In the context of ecological risk assessment, the approach provides a valuable tool for the problem formulation stage in risk analysis (U.S. Environmental Protection Agency 1992, Hayes et al. 2007). The graphical nature of the underlying dynamical model, in particular, lends a common symbolic language capable of capturing the understanding and opinions of researchers and stakeholders across a broad array of disciplines (Dambacher et al. 2007). This approach thus documents and enhances understanding in systems that are poorly understood, difficult to quantify, or both.

ACKNOWLEDGMENTS

We appreciate the constructive comments and suggestions given by our colleagues Jane Jorgensen, Bruce D'Ambrosio, Jonathan Rhodes, Philippe Rossignol, and Simon Barry. G. R. Hosack acknowledges support from an NSF IGERT graduate fellowship in Ecosystem Informatics (NSF award 0333257). K. R. Hayes and J. M. Dambacher were partially supported by Australian Centre for Excellence in Risk Assessment Project No. 06/01.

LITERATURE CITED

- Bender, E. A., T. J. Case, and M. E. Gilpin. 1984. Perturbation experiments in community ecology: theory and practice. *Ecology* 65:1–13.
- Berlow, E. L., et al. 2004. Interaction strengths in food webs: issues and opportunities. *Journal of Animal Ecology* 73: 585–598.
- Borer, E. T., C. J. Briggs, W. W. Murdoch, and S. L. Swarbrick. 2003. Testing intraguild predation theory in a field system: does numerical dominance shift along a gradient of productivity? *Ecology Letters* 6:929–935.
- Borer, E. T., W. W. Murdoch, and S. L. Swarbrick. 2004. Parasitoid coexistence: linking spatial field patterns with mechanism. *Ecology* 85:667–678.
- Borusk, M. E., C. A. Stow, and K. H. Reckhow. 2004. A Bayesian network of eutrophication models for synthesis, prediction, and uncertainty analysis. *Ecological Modelling* 173:219–239.
- Burger, J. A., and M. Gochfeld. 1997. Paradigms for ecological risk assessment. *Annals of the New York Academy of Sciences* 837:372–86.
- Burgman, M. A. 2005. Risks and decisions for conservation and environmental management. University Press, Cambridge, UK.
- Cain, J. 2001. Planning improvements in natural resource management. Centre for Ecology and Hydrology, Wallingford, UK.
- Dambacher, J. M., D. T. Brewer, D. M. Dennis, M. Macintyre, and S. Foale. 2007. Qualitative modelling of gold mine impacts on Lihir Island's socioeconomic system and reef-edge fish community. *Environmental Science and Technology* 41:555–562.
- Dambacher, J. M., R. Levins, and P. A. Rossignol. 2005. Life expectancy change in perturbed communities: derivation and qualitative analysis. *Mathematical Biosciences* 197:1–14.
- Dambacher, J. M., H. W. Li, and P. A. Rossignol. 2002. Relevance of community structure in assessing indeterminacy of ecological predictions. *Ecology* 83:1372–1385.
- Dambacher, J. M., H. W. Li, and P. A. Rossignol. 2003a. Qualitative predictions in model ecosystems. *Ecological Modelling* 161:79–93.
- Dambacher, J. M., H. K. Luh, H. W. Li, and P. A. Rossignol. 2003b. Qualitative stability and ambiguity in model ecosystems. *American Naturalist* 161:876–888.
- Dojer, N., A. Gambin, A. Mizera, B. Wilczynski, and J. Tiuryn. 2006. Applying dynamic Bayesian networks to perturbed gene expression data. *BMC Bioinformatics* 7:249.
- Emmerson, M., and J. M. Yearsley. 2004. Weak interactions, omnivory and emergent food-web properties. *Proceedings of the Royal Society of London Series B* 271:397–405.
- Fairbrother, A., and J. G. Turnley. 2005. Predicting risks of uncharacteristic wildfires: application of the risk assessment process. *Forest Ecology and Management* 211:28–35.
- Ferson, S. 1996. What Monte Carlo methods cannot do. *Human and Ecological Risk Assessment* 2:990–1007.
- Francis, R. I. C. C., and R. Shotton. 1997. "Risk" in fisheries management: a review. *Canadian Journal of Fisheries and Aquatic Sciences* 54:1699–1715.
- Hayes, K. R. 2002. Identifying hazards in complex ecological systems. Part 2. Infections modes and effects analysis for biological invasions. *Biological Invasions* 4:251–261.
- Hayes, K. R., A. R. Kapuscinski, G. Dana, L. Sifa, and R. H. Devlin. 2007. Introduction to environmental risk assessment for transgenic fish. Pages 1–28 in A. R. Kapuscinski, K. R. Hayes, S. Li, and G. Dana, editors. Environmental risk assessment of genetically modified organisms. Volume 3: methodologies for transgenic fish. CABI Publishing, Oxfordshire, UK.
- Hoffman, E. O., and J. S. Hammonds. 1994. Propagation of uncertainty in risk assessments: the need to distinguish between uncertainty due to lack of knowledge and uncertainty due to variability. *Risk Analysis* 14:707–712.
- Hulot, F. D., G. Lacroix, F. Lescher-Moutoué, and M. Loreau. 2000. Functional diversity governs ecosystem response to nutrient enrichment. *Nature* 405:340–344.
- Levins, R. 1974. The qualitative analysis of partially specified systems. *Annals of the New York Academy of Sciences* 231: 123–138.
- Levins, R. 1998. Qualitative mathematics for understanding, prediction, and intervention in complex systems. Pages 178–204 in D. Rapport, R. Costanza, P. R. Epstein, C. Gaudet, and R. Levins, editors. Ecosystem health. Blackwell Science, Malden, Massachusetts, USA.
- Luck, R. F., and H. Podoler. 1985. Competitive exclusion of *Aphytis lingnanensis* by *A. melinus*: potential role of host size. *Ecology* 66:904–913.
- Marcot, B. G., R. S. Holthausen, M. G. Raphael, M. M. Rowland, and M. J. Wisdom. 2001. Using Bayesian belief networks to evaluate fish and wildlife population viability under land management alternatives from an environmental impact statement. *Forest Ecology and Management* 153: 29–42.
- May, R. M. 1974. Stability and complexity in model ecosystems. Second edition. Princeton University Press, Princeton, New Jersey, USA.
- Metropolis, N., and S. Ulam. 1949. The Monte Carlo method. *Journal of the American Statistical Association* 44:335–341.
- Minc, H. 1978. Permanents. *Encyclopedia of mathematics and its applications*. Volume 6. Addison-Wesley Publishing Company, Reading, UK.
- Morgan, M. G., and M. Henrion. 1990. Uncertainty: a guide to dealing with uncertainty in quantitative risk and policy

- analysis. Cambridge University Press, Melbourne, Victoria, Australia.
- Mortera, J., A. P. Dawid, and S. L. Lauritzen. 2003. Probabilistic expert systems for DNA mixture profiling. *Theoretical Population Biology* 63:191–205.
- Murdoch, W., C. J. Briggs, and S. Swarbrick. 2005. Host suppression and stability in a parasitoid–host system: experimental demonstration. *Science* 309:610–613.
- Office of the Gene Technology Regulator. 2005. Risk analysis framework. Department of Health and Ageing, Australian Government, Canberra, Australia.
- Ong, I. M., J. D. Glasner, and D. Page. 2002. Modelling regulatory pathways in *E. coli* from time series expression profiles. *Bioinformatics* 18(S1):S241–S248.
- Pearl, J. 2000. *Causality: models, reasoning, and inference*. Cambridge University Press, New York, New York, USA.
- Pollino, C. A., O. Woodberry, A. Nicholson, K. Korb, and B. T. Hart. 2007. Parameterisation and evaluation of a Bayesian network for use in an ecological risk assessment. *Environmental Modelling and Software* 22:1140–1152.
- Punt, A. E., and R. Hilborn. 1997. Fisheries stock assessment and decision analysis: the Bayesian approach. *Reviews in Fish Biology and Fisheries* 7:35–63.
- Reckhow, K. H. 1994. Water quality simulation modelling and uncertainty analysis for risk assessment and decision making. *Ecological Modelling* 72:1–20.
- Regan, H. M., M. Colyvan, and M. A. Burgman. 2002. A taxonomy and treatment of uncertainty for ecology and conservation biology. *Ecological Applications* 12:618–628.
- Ruckelshaus, M. H., P. Levin, J. B. Johnson, and P. M. Kareiva. 2002. The Pacific salmon wars: what science brings to the challenge of recovering species. *Annual Review of Ecology and Systematics* 33:66–706.
- Shiple, B. 2000. *Cause and correlation in biology*. Cambridge University Press, Cambridge, UK.
- Stiber, N. A., M. J. Small, and M. Pantazidou. 2004. Site-specific updating and aggregation of Bayesian Belief Network models for multiple experts. *Risk Analysis* 24:1529–1538.
- Ticehurst, J. L., L. T. H. Newham, D. Rissik, R. A. Letcher, and A. J. Jakeman. 2007. A Bayesian network approach for assessing the sustainability of coastal lakes in New South Wales, Australia. *Environmental Modelling and Software* 22:1129–1139.
- U.S. Environmental Protection Agency. 1992. Framework for ecological risk assessment. EPA/630/R-92/001. Risk Assessment Forum, Washington, D.C., USA.
- Varis, O., and S. Kuikka. 1999. Learning Bayesian decision analysis by doing: lessons from environmental and natural resources management. *Ecological Modelling* 119:177–195.
- Wootton, J. T., and M. Emmerson. 2005. Measurement of interaction strength in nature. *Annual Review of Ecology, Evolution, and Systematics* 36:419–444.
- Yodzis, P. 1988. The indeterminacy of ecological interactions as perceived through perturbation experiments. *Ecology* 69:508–515.
- Yu, D. S., R. F. Luck, and W. W. Murdoch. 1990. Competition, resource partitioning and coexistence of an endoparasitoid *Encarsia perniciosi* and an ectoparasitoid *Aphytis melinus* of the California red scale. *Ecological Entomology* 15:469–480.

APPENDIX

Methods and results for second-order Monte Carlo simulation exploring the reliability of prediction weights given different distribution shapes and dependence among elements of **A** (*Ecological Archives* A018-035-A1).

SUPPLEMENT

Maple file for constructing conditional probability tables from signed directed graphs, SDG graphical editor program, example BBNS for the parasitoid and lake mesocosm studies, and instruction guide for SDG-BBN construction (*Ecological Archives* A018-035-S1).